Fundamental limits on the rate of bacterial cell division

Nathan M. Belliveau[†, 1], **Griffin Chure**[†, 2, 3], **Christina L. Hueschen**[4], **Hernan G. Garcia**[5], **Jane Kondev**[6], **Daniel S. Fisher**[7], **Julie A. Theriot**[1, 8], **Rob Phillips**[2, 9, *]

***For correspondence:**

[†]These authors contributed equally to this work

[1]Department of Biology, University of Washington, Seattle, WA, USA; [2]Division of Biology and Biological Engineering, California Institute of Technology, Pasadena, CA, USA; [3]Department of Applied Physics, California Institute of Technology, Pasadena, CA, USA; [4]Department of Chemical Engineering, Stanford University, Stanford, CA, USA; [5]Department of Molecular Cell Biology and Department of Physics, University of California Berkeley, Berkeley, CA, USA; [6]Department of Physics, Brandeis University, Waltham, MA, USA; [7]Department of Applied Physics, Stanford University, Stanford, CA, USA; [8]Allen Institute for Cell Science, Seattle, WA, USA; [9]Department of Physics, California Institute of Technology, Pasadena, CA, USA; [*]Contributed equally

Abstract This will be written next (promise).

Translation and Ribosomal Synthesis

Lastly, we turn our attention to the process of synthesizing new proteins, translation. This process stands as a good candidate for potentially limiting growth since the synthesis of new proteins relies on the generation of ribosomes, themselves proteinaceous molecules. As we will see in the coming sections of this work, this poses a "chicken-or-the-egg" problem where the synthesis of ribosomes requires ribosomes in the first place.

We will begin our exploration of protein translation in the same spirit as we have in previous sections – we will draw order-of-magnitude estimates based on our intuition and available literature, and then compare these estimates to the observed data. In doing so, we will estimate both the absolute number of ribosomes necessary for replication of the proteome as well as the synthesis of amino-acyl tRNAs. From there we consider the limitations on ribosomal synthesis in light of our estimates on both the synthesis of ribosomal proteins and our earlier results on rRNA synthesis.

tRNA Synthetases

We begin by first estimating the number of tRNA synthetases in *E. coli* needed to convert free amino-acids to polypeptide chains. At a doubling time of $\approx$ 5000 s, *E. coli* has roughly 3×10^6 proteins per cell (BNID: 115702; ***Milo et al.*** (***2010***)). Assuming that the typical protein is on the order of $\approx$ 300 amino acids in length (BNID: 100017; ***Milo et al.*** (***2010***)), we can estimate that a total of $\approx 10^9$ amino acids are stitched together by peptide bonds.

How many tRNAs are needed to facilitate this remarkable number of amino acid delivery events to the translating ribosomes? It is important to note that tRNAs are recycled after they've passed through the ribosome and can be recharged with a new amino acid, ready for another round of peptide bond formation. While some *in vitro* data exists on the turnover of tRNA in *E. coli* for different amino acids, we can make a reasonable estimate by comparing the number of amino acids to be polymerized to cell division time. Using our stopwatch of 5000 s and 10^9 amino acids,

we arrive at a requirement of $\approx 2 \times 10^5$ tRNA molecules to be consumed by the ribosome per second.

There are many processes which go into synthesizing a tRNA and ligating it with the appropriate amino acids. As we discussed previously, there appear to be more than enough RNA polymerases per cell to synthesize the needed pool of tRNAs. Without considering the many ways in which amino acids can be scavenged or synthesized *de novo*, we can explore ligation the as a potential rate limiting step. The enzymes which link the correct amino acid to the tRNA, known as tRNA synthetases or tRNA ligases, are incredible in their proofreading of substrates with the incorrect amino acid being ligated once out of every 10^4 to 10^5 times (BNID: 103469, ***Milo et al.*** (***2010***)). This is due in part to the consumption of energy as well as a multi-step pathway to ligation. While the rate at which tRNA is ligated is highly dependent on the identity of the amino acid, it is reasonable to state that the typical tRNA synthetase has charging rate of $\approx$ 20 AA per tRNA synthetase per second (BNID: 105279, ***Milo et al.*** (***2010***)).

We can make an assumption that aminio-acyl tRNAs are in steady-state where they are produced at the same rate they are consumed, meaning that 2×10^5 tRNAs must be charged per second. Combining these estimates together, as shown schematically in ***Figure 1***(A), yields an estimate of $\approx 10^4$ tRNA synthetases per cell with a division time of 5000 s. This point estimate is in very close agreement with the observed number of synthetases (the sum of all 20 tRNA synthetases in *E. coli*). This estimation strategy seems to adequately describe the observed growth rate dependence of the tRNA synthetase copy number (shown as the grey line in ***Figure 1***(B)), suggesting that the copy number scales with the cell volume.

In total, the estimated and observed $\approx 10^4$ tRNA synthetases occupy only a meager fraction of the total cell proteome, around 0.5% by abundance. It is reasonable to assume that if tRNA charging was a rate limiting process, cells would be able to increase their growth rate by devoting more cellular resources to making more tRNA synthases. As the synthesis of tRNAs and the corresponding charging can be highly parallelized, we can argue that tRNA charging is not a rate limiting step in cell division, at least for the growth conditions explored in this work.

Protein Synthesis

With the number of tRNA synthetases accounted for, we now consider the abundance of the protein synthesis machines themselves, ribosomes. Ribosomes are enormous protein/rRNA complexes that facilitate the peptide bond formation between amino acids in the correct sequence as defined by the coding mRNA. Before we examine the synthesis of the ribosome proteins and the limits that may place on the observed bacterial growth rates, let's consider replication of the cellular proteome.

As described in the previous section, an *E. coli* cell consisting of of $\approx 3\times10^6$ proteins will have on the order $\approx 10^9$ peptide bonds per proteome. While the rate at which ribosomes translates is well known to have a growth rate dependence ***Dai et al.*** (***2018***) and is a topic which we discuss in detail in the coming sections. However, for the purposes of our order-of-magnitude estimate, we can make the approximation that translation occurs at a rate of $\approx$ 15 amino acids per second per ribosome (BNID: 100233, ***Milo et al.*** (***2010***)). Under this approximation and assuming a division time of 5000 s, we can arrive at an estimate of $\approx 10^4$ ribosomes are needed to replicate the cellular proteome, shown in ***Figure 1***(B). This point estimate, while glossing over important details such as chromosome copy number and growth-rate dependent translation rates, proves to be notably accurate when compared to the experimental observations (***Figure 1***(B)).

Translation and Ribosomal Synthesis as a Growth-Rate Limiting Step

Thus far, the general back-of-the-envelope estimates have been reasonably successful in explaining what sets the scale of absolute protein copy number as well as their observed dependence on the cellular growth rate. A recurring theme that has arisen is the ability of cells to parallelize their biosynthesis tasks. For example, while DNA replication speed-limit is $\approx$ 40 minutes to repli-

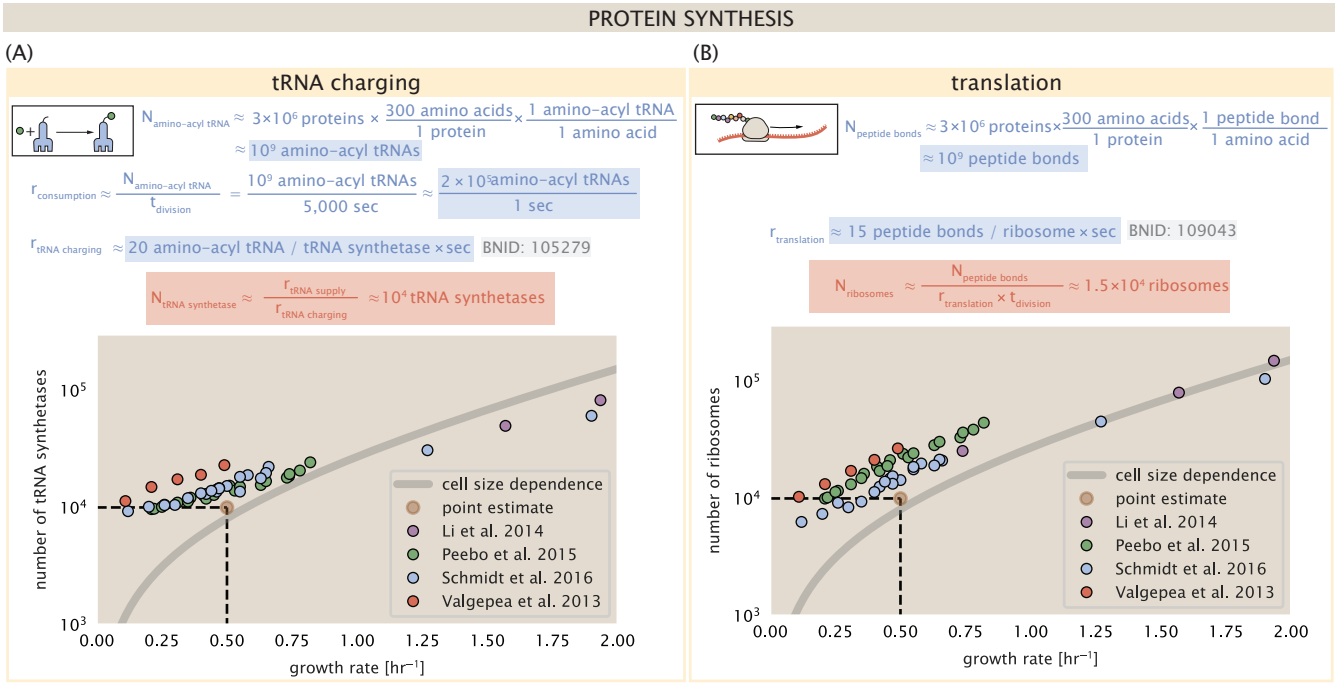

Figure 1. Estimation of the required tRNA synthetases and ribosomes. (A) Estimation for the number of tRNA synthetases that will supply the required amino acid demand. The sum of all tRNA synthetases copy numbers are plotted as a function of growth rate ([ArgS], [CysS], [GlnS], [GltX], [IleS], [LeuS], [ValS], $[AlaS]_2$, $[AsnS]_2$, $[AspS]_2$, $[TyrS]_2$, $[TrpS]_2$, $[ThrS]_2$, $[SerS]_2$, $[ProS]_2$, $[PheS]_2[PheT]_2$, $[MetG]_2$, $[lysS]_2$, $[HisS]_2$, $[GlyS]_2[GlyQ]_2$). (B) Estimation of the number of ribosomes required to synthesize 10^9 peptide bonds with an elongation rate of 15 peptide bonds per second. The average abundance of ribosomes is plotted as a function of growth rate. Our estimated values are shown for a growth rate of 0.5 hr^{-1}. Grey lines correspond to the estimated complex abundance calculated at different growth rates. See Supplemental Information XX for a more detail description of this calculation.

cate a genome, cells can divide faster than this by initiating more than one round of replication per doubling. The process of protein synthesis overall doesn't appear to be rate-limiting, since for example, cells are able to induce the expression of additional enzymes to grow on alternative carbon sources. However, as we will see, the synthesis of ribosomal proteins presents a special case where parallelization is not possible (***Figure 2***(A)). Thus, it is plausible that translation may be a key factor in determining the cellular growth rate.

To gain some intuition into how translation can set the speed of bacterial growth, we again consider the total number of peptide bonds that must be synthesized, which we denote as N_{pep}. With cells growing exponentially in time (***Godin et al., 2010***), we can compute the number of amino acids to be polymerized as

$$N_{\text{pep}}\lambda = r_t R f_a, \tag{1}$$

where λ is the cell growth rate in s^{-1}, r_t is the maximum elongation rate in AA·s^{-1}, and R is the average ribosome copy number per cell. The addition factor f_a refers to the fraction of actively translating ribosomes, and allows us to account for the possibility of nonfunctional, immature ribosomes or active sequestration of ribosomes mediated by the secondary-messenger molecule alarmones, guanosine pentaphosphate [(p)ppGpp] at slow growth (***Dennis et al., 2004***; ***Dai et al., 2016***). Knowing the number of peptide bonds to be formed permits us to compute the translation-limited growth rate as

$$\lambda_{\text{translation-limited}} = \frac{r_t R f_a}{N_{\text{pep}}}. \tag{2}$$

Alternatively, since N_{pep} is related to the total protein mass through the molecular weight of each protein, we can also consider the growth rate in terms of the fraction of the total proteome mass dedicated to ribosomal proteins. By making the approximation that an average amino acid has a molecular weight of 110 Da (BNID: 104877, ***Milo et al.*** (***2010***)), the total protein mass m_{protein} is related to N_{AA} by $(m_{\text{protein}}/110\text{ Da})\times N_A$, where N_A is Avogadro's number. Similarly, R is related to the ribosomal protein mass by $R \approx (m_R/800\text{ Da}) \times N_A$, where 800 Da reflects the summed molecular weight of all ribosomal subunits. This allows us to approximate $R/N_{\text{pep}} \approx \Phi_R/L_R$, where Φ_R is the ribosomal mass fraction m_{protein}/m_R, and L_R the ratio of 800 kDa / 110 Da per amino acid or, alternatively, the total length in amino acids that make up a ribosome. The translation-limited growth rate can then be written in the form

$$\lambda_{\text{translation-limited}} \approx \frac{r_t}{L_R}\Phi_R f_a. \tag{3}$$

This is plotted as a function of ribosomal fraction Φ_R in ***Figure 2***(B), where we take L_R = 7459 AA, corresponding to the length in amino acids for all ribosomal subunits of the 50S and 30S complex (BNID: 101175, (***Milo et al., 2010***)), and f_a = 1.

The growth rate defined by ***Equation 3*** reflects mass-balance under steady-state growth and has long provided a rationalization of the apparent linear increase in *E. coli*'s ribosomal content as a function of growth rate (***Maaløe, 1979***; ***Scott et al., 2010***). Here we see that there will be a maximum rate when Φ_R = 1, which for a translation rate of 17 amino acids per second, gives us $\lambda \approx 8\,\text{hr}^{-1}$, or a doubling time just under 6 minutes (***Figure 2***(B), dashed line). Interestingly, this limit is independent of the absolute number of ribosomes and is simply given by the time to translate an entire ribosome, L_R/r_t. As shown in ***Figure 2***(A), we can reconcile this with the observation that in order to double the average number of ribosomes, each ribosome must produce a second ribosome and this process cannot be parallelized. Unless protein synthesis can increase, or cells can trim their total ribosomal protein mass, this must represent an absolute speed limit for cell doubling.

In recent work from ***Dai et al.*** (***2016***), the authors made independent measurements of r_t, Φ_R (via RNA-to-protein ratios, and directly by mass spectrometry), and growth rate, enabling inference of the active fraction f_a across the entire range of growth rates considered here. In **??**() we use this measurement of f_a to estimate the active fraction of ribosomal protein across the proteomic data

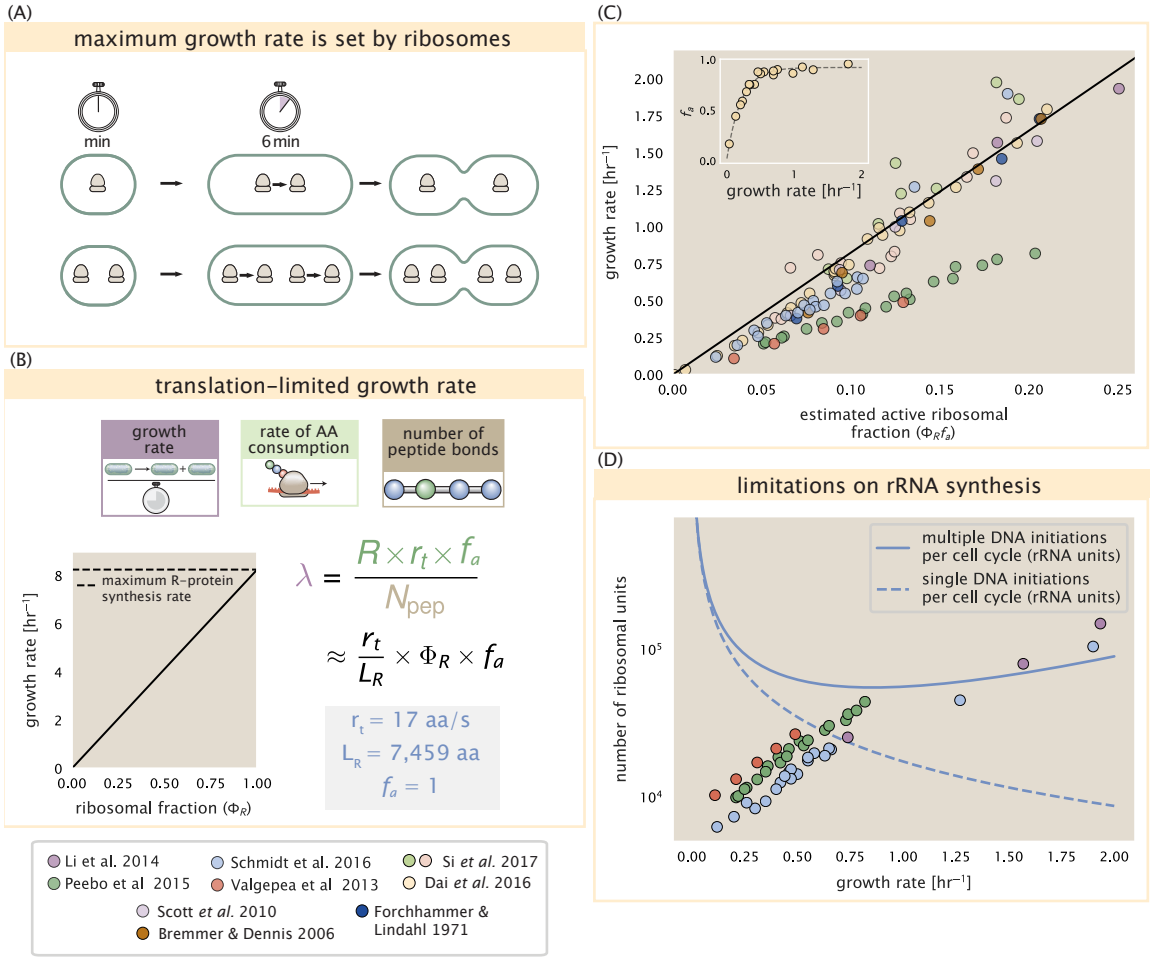

Figure 2. Translation-limited growth rate. (A) An inherent maximum growth rate is set by the time to synthesize all ribosomal subunits. This growth rate is given by r_t/L_R, where r_t is the elongation rate and L_R is the total number of amino acids that make up the entire ribosomal complex. This rate is independent of the number of ribosomes; instead limited serial requirement for each ribosome to double itself. (B) Translation-limited growth as a function of the ribosomal fraction. The solid line is calculated for an elongation rate of 17 aa per second. The dashed line corresponds to the maximum rate of ribosomal protein (R-protein) synthesis considered in part (A). (C) Actively translating ribosomal fraction versus growth rate. The actively translating ribosomal fraction is calculated using the estimated values of f_a from ***Dai et al.*** (***2016***) (shown in inset; see Supplemental Section XX for additional detail). (D) Maximum number of rRNA units that can be synthesized as as a function of growth rate. Solid curve corresponds to the rRNA copy number is calculated by multipyling the number of rRNA operons by the estimated number of ⟨# ori⟩ at each growth rate. The quantity ⟨# ori⟩ was calculated using Equation 4 and the measurements from ***Si et al.*** (***2017***) that are plotted in ***Figure 3***(A). The dashed line shows the maximal number of functional rRNA units produced from a single chromosomal initiation per cell cycle.

sets. Importantly, we find that from the perspective of actively translating ribosomes, cells are effectively skirting the limit in growth rate that is set by ***Equation 3***, as nutrient conditions vary.

Earlier, we considered rRNA synthesis (see Section **RNA Synthesis**), finding that, when the rRNA operons are maximally loaded with RNA polymerase, the cell can produce ≈ 1 functional rRNA unit per second per operon. In ***Figure 2***(C), we show the maximum number of ribosomes that could be made as a function of growth rate given this rRNA production rule-of-thumb. While each *E. coli* genome has 7 copies of the rRNA operon (BNID: 107866, ***Milo et al.*** (***2010***)), parallelization of DNA synthesis by firing multiple rounds of replication at a time can drastically the effective number of rRNA operons. The blue curve in ***Figure 2***(C), we assume that the effective number of rRNA operons increases in proportion to the number of origins of replication $\langle$# ori$\rangle$ (solid blue line; with the calculation of $\langle$# ori$\rangle$ described in the next section). Although we expect this value to drastically overestimate rRNA abundance at slower growth rates ($\lambda < 0.5\,\mathrm{hr}^{-1}$), it provides a useful reference when considered along with the proteomic measurements that are also plotted. For growth rates above about 1 hr^{-1}, we find that cells will need to transcribe rRNA near their maximal rate. The dashed blue curve in ***Figure 2***(C) shows the maximal number of functional rRNA units that could be synthesized from a single genome (ignoring the chromosome replication speed limit of $\approx$ 40 minutes per genome). The convergence between the maximum rRNA production with parallelization and the experimentally measured ribosome copy number (points in ***Figure 2***(C)), suggests rRNA synthesis may begin to present a bottleneck in cell division at the fastest growth rates. While this strain of *E. coli* is rarely reported to grow faster than 2 hr^{-1}, other bacteria with more copies of rRNA genes have been found that surpass this growth rate (***Bremer and Dennis, 2008***; ***Roller et al., 2016***).

Relationship Between Cell Size and Growth Rate

The relationship between cell size and growth rate has long been of interest in the study of bacterial physiology, particularly following the now six decade-old observation that cell volume appears to increase exponentially with growth rate; known as Schaechter's growth law (***Schaechter et al., 1958***; ***Taheri-Araghi et al., 2015***). However, the mechanism that governs this relationship, and even the question of whether the change in average cell size is truly exponential, has remained under debate (***Harris and Theriot, 2018***). Given the importance of cell size in determining the total protein mass that must be doubled (as well as in setting other parameters like the surface-area-to-volume ratio), we examine the influence size may have in setting the scales of protein abundance and growth dependence observed in the proteomic datasets.

As shown in ***Figure 2***(B), cells grow at a near-maximal rate dictated by their total ribosomal mass fraction Φ_R, at least at moderate growth rates above 0.5 hr^{-1}, suggesting that growth rate could increased simply by making more ribosomes and increasing Φ_R. In reality, however, large swaths of the proteome increase in absolute protein abundance as cells grow faster (Supplemental Figure X), and the ability to add additional ribosomes is likely constrained by other factors including crowding due to their large size (***Delarue et al., 2018***; ***Soler-Bistué et al., 2020***). Rather, it is well-documented that *E. coli* cells add a constant volume per origin of replication (termed a "unit cell" or "initiation mass"), which is robust to a remarkable array of cellular perturbations (***Si et al., 2017***). To consider this in the context of the proteomic data, we used the measurements from ***Si et al.*** (***2017***) for wild-type *E. coli* cells grown in different nutrient conditions (***Figure 3***(A)) to estimate the average number of origins per cell $\langle$# ori$\rangle$ across the data. Indeed, we find an approximately linear correlation between ribosome copy number and $\langle$# ori$\rangle$ (***Figure 3***(B)).

The average number of origins $\langle$# ori$\rangle$ is set by how often replication must be initiated per cell doubling under steady-state growth. This can be quantified as

$$\langle \text{\# ori} \rangle = 2^{\tau_{cyc}/\tau} = 2^{\tau_{cyc}\lambda/ln(2)}, \tag{4}$$

where t_{cyc} is the cell cycle time (referring to the time from replication initiation to cell division), and τ is the cell doubling time. For a constant cell cycle time, observed at growth rates above about 0.5

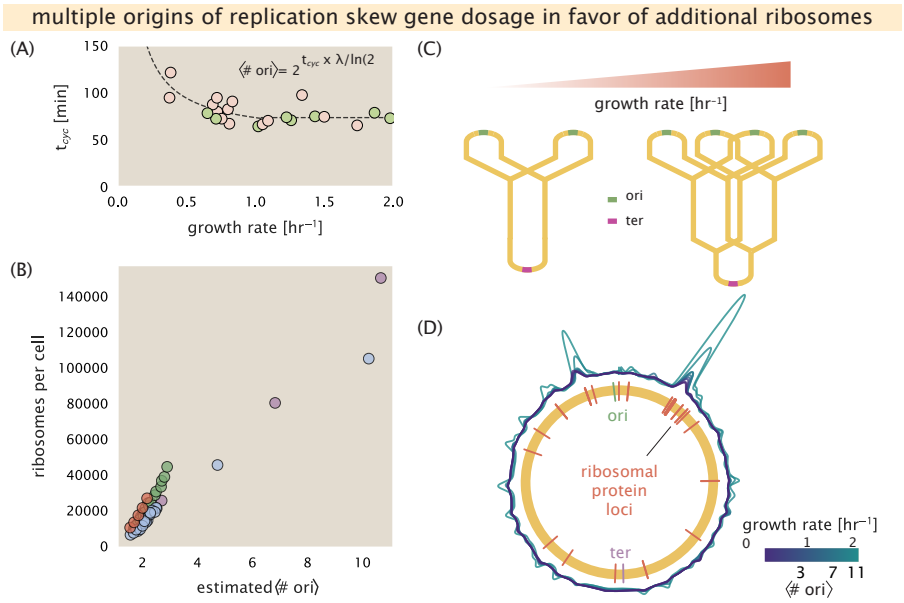

Figure 3. Multiple replication initiations bias protein synthesis in favor of more ribosome. (A) Experimental data from Si *et al.* (2017). Dashed line shows fit to the data, which were used to estimate ⟨# ori⟩. t_{cyc} was assumed to vary in proportion to τ for doubling times great than 40 minutes, and then reach a minimum value of [fill in] minutes below this (see Supplemental Appendix X for additional details). Red data points correspond to measurements in strain MG1655, while light green points are for strain NCM3722. (B) Plot of the ribosome copy number estimated from the proteomic data against the estimated ⟨# ori⟩. (C) Schematic shows the expected increase in replication forks (or number of ori regions) as *E. coli* cells grow faster. (D) A running Gaussian average (20 kbp st. dev.) of protein copy number is calculated for each growth condition considered by (***Schmidt et al., 2016***). Since total protein abundance increases with growth rate, protein copy numbers are median-subtracted to allow comparison between growth conditions. ⟨# ori⟩ are estimated using the data in (A) and Equation 4. [still looking into how best to use this type of analysis]

hr^{-1} (***Helmstetter and Cooper, 1968***), ***Equation 4*** states that ⟨# ori⟩ will increase exponentially with the growth rate.

Why does *E. coli* add a constant volum eper ⟨# ori ⟩? To gain insight on this phenomenological discovery and how it pertains to growth, we must consider how the protome size and composition changes with respect to growth rate. In ***Figure 3***(D), we consider the position-dependent protein expression across the chromosome for each of the growth conditions from ***Schmidt et al.*** (***2016***). Here, we calculated a running Gaussian average of protein copy number (20 kbp st. dev. averaging window) based on each gene's transcriptional start site, which were then median-subtracted to account for the differences in total protein abundance with each growth condition. Importantly, we find that the major deviations in protein copy number are largely restricted to regions of ribosomal protein genes, with substantially higher deviations observed for cells with high ⟨# ori⟩ (teal), as compared to those with low ⟨# ori⟩ (purple). This is particularly apparent for genes closer to the origin, where the majority of ribosomal proteins are found. This suggests that in addition to the linear scaling between protein abundance and ⟨# ori⟩, the relative ribosomal abundance is tuned in proportion to ⟨# ori⟩. Since growth rate depends specifically on the ribosomal fraction Φ_R, this result suggests that cells are changing their size as a way to tune Φ_R to match the available nutrient conditions.

Alarmone-Mediated Regulation Controls the Rate of Protein Synthesis

As we have seen, cell size, number of actively translating ribosomes, and cellular growth rate are intimately connected. This provides a mechanistic framework through which we can understand how cellular physiology is tuned to match biosynthetic capacity to the nutrient conditions of the

environment. Take, for example, the recent experimental work by ***Dai et al.*** (***2016***) which measured the perturbation to these key cellular phenotypes resulting from deletion of the primary glucose transport system in *E. coli*. In this deletion background, *both* cellular growth rate *and* the ribosome mass fraction of the proteome decreased by a factor of two relative to a strain with wild-type levels of the glucose transporters. This factor of two decrease in growth rate is agreement with the intuition provided by ***Equation 3*** for a ribosome mass fraction decrease of this magnitude. In the final section of this work, we explore the interconnection between cell size, ribosome content, and growth rate from a mathematical perspective, resulting in a minimal model of growth rate regulation given the nutrient conditions of the growth medium.

To react to changes in nutrient conditions, bacteria rely on the synthesis or degradation of secondary-messenger molecules termed alarmones like guanosine pentaphosphate [(p)ppGpp], which result in changes to the global transcriptional and translational activity. In *E. coli*, amino acid starvation causes the accumulation of de-acylated tRNAs at the ribosome's A-site, leading to a strong increase in (p)ppGpp synthesis activity by the enzyme RelA(***Hauryliuk et al., 2015***). The accumulation of (p)ppGpp regulates the fraction of the ribosome pool which is actively translating, f_a. The concentration of (p)ppGpp increases as growth rate is slowed (with $f_a \approx 0.5$ at a growth rate of ≈ 0.3 hr^{-1}), indicating that regulation of ribosome activity is linked to coordinating growth in poor nutrient conditions.

Furthermore, (p)ppGpp can inhibit the initiation of DNA replication by mediating a change in transcriptional activity and the supercoiling state of the origin of replication (***Kraemer et al., 2019***). These observations all raise the possibility that, via (p)ppGpp, cells mediate the growth-rate dependent changes in $\langle$# ori$\rangle$, cell size and ribosomal abundance (***Zhu and Dai, 2019***; ***Büke et al., 2020***). Indeed, recent work in a (p)ppGpp deficient strain of *E. coli* found that cells exhibited a high ratio of $\langle$# ori$\rangle$ to $\langle$# ter$\rangle$ and cell size that was more consistent with a fast growth state where (p)ppGpp levels are normally low (***Fernández-Coll et al., 2020***).

Ribosomal Elongation Rate and Cellular Growth Rate are Linked by Amino Acid Scarcity

To better understand how cells are able to maximize their growth rate under different degrees of nutrient limitation, we consider a mode of regulation in which the rate of peptide elongation r_t depends only on the availability of amino acids (and, therefore, also amino-acyl tRNAs). As the rate of amino acid supply r_{AA} decreases, slowing the rate of elongation provides a means by which the cell can tune the rate of amino acid consumption (mathematized as $r_t \times R \times f_a$) to remain in steady-state growth, shown schematically in ***Figure 4***(A). Under this simplistic model, other molecular players required for translation like elongation factors and GTP are considered in sufficient abundance, which appear to be valid assumptions given our analysis of the proteomic data and energy production thus far.

For simplicity, we consider all amino acids as a single species with an effective cellular concentration $[AA]_{\text{eff}}$. The rate of elongation r_t will depend on how quickly the ribosomes can match codons with their correct amino-acyl tRNA, along with the subsequent steps of peptide bond formation and translocation. We therefore coarse-grain the steps of elongation to two time-scales, 1) the time required to find and bind each correct amino-acyl tRNA, and 2) the remaining steps in peptide elongation that will not depend on the amino acid availability. The time to translate each codon is given by the inverse of the elongation rate r_t, which can be written as,

$$\frac{1}{r_t} = \frac{1}{k_{on}\alpha[AA]_{\text{eff}}} + \frac{1}{r_t^{\text{max}}}. \tag{5}$$

where we have assumed that the rate of binding by amino-acyl tRNA k_{on} is proportional to $[AA]_{\text{eff}}$ by a constant α. The second term on the right-hand side reflects our assumption that other steps in peptide elongation are not rate-limiting, with a maximum elongation rate r_t^{max} of about 17 amino

acids per second ***Dai et al.*** (***2016***). This can be stated more succinctly in terms of an effective dissociation constant,

$$K_D = \frac{r_t^{\max}}{\alpha k_{\text{on}}}, \tag{6}$$

where the elongation rate r_t is now given by

$$r_t = \frac{r_t^{\max}}{1 + K_D/[AA]_{\text{eff}}}. \tag{7}$$

Under steady-state growth, the amino acid concentration is constant ($\frac{d[AA]_{\text{eff}}}{dt} = 0$), meaning that synthesis and consumption are matched. The effective amino acid concentration $[AA]_{\text{eff}}$ will relate to the rate of amino acid synthesis (or import, for rich media) and/or tRNA charging, as r_{AA}, and the rate of consumption, $r_t \times R \times f_a$ by,

$$\int_0^t \frac{d[AA]_{\text{eff}}}{dt} dt = \int_0^t ([r_{AA}] - [r_t \times R \times f_a]) dt, \tag{8}$$

where the time from 0 to t is an arbitrary length of time, and the square brackets indicate concentrations per unit time. Integrating ***Equation 8*** yields.

$$[AA]_{\text{eff}} = t([r_{AA}] - [r_t \times R \times f_a]). \tag{9}$$

Alternatively, we can state this in terms of absolute ribosome copy number R by considering a unit volume V,

$$[AA]_{\text{eff}} = \frac{t(r_{AA} - r_t \times R \times f_a)}{V}, \tag{10}$$

where r_{AA} is in units of AA per unit time and r_t is in units of AA per unit time per ribosome. With an expression for $[AA]_{\text{eff}}$ in hand, we can now solve ***Equation 7*** for r_t which is a quadratic function with a physically-meaningful positive root of

$$r_t = \frac{-t(r_{AA} + r_t^{(\max)} R f_a) - K_D V \pm \sqrt{(r_{AA} t + r_t^{(\max)} R f_a t + K_D V)^2 - 4(R f_a t)(r_t^{(\max)} r_{AA} t)}}{-2 R f_a t}. \tag{11}$$

In ***Figure 4***(B), we illustrate how the elongation rate depends on the ribosomal copy number. Here, we have considered a unit volume $V = 1\mu\text{m}^3$, a unit time $t = 1$ s, a $K_D = 5$ mM (inferred from ***Bennett et al.*** (***2009***)), $f_a = 1$, and an arbitrarily chosen $r_{AA} = 5 \times 10^6$ AA $\cdot$ s$^{-1}\cdot$ μm^{-3}. At low ribosome copy numbers, the observed elongation rate is dependent primarily on the ratio of $K_D/V r_{AA}$ [as $r_t^{\max} \times R \times f_a << r_{AA}$, point (1) in ***Figure 4***(B)]. As the ribosome copy number is increased such that the amino acid supply rate and consumption rate are nearly equal [point (2) in ***Figure 4***(B)], the observed elongation rate begins to decrease sharply. When the ribosome copy number is increased even further, consumption at the maximum elongation rate exceeds the supply rate, yielding a significantly reduced elongation rate [point (3) in ***Figure 4***B)]. While the elongation rate will always be dominated by the amino acid supply rate at sufficiently low ribosome copy numbers, the elongation rate at larger ribosome abundances can be increased by tuning f_a such that not all ribosomes are elongating, reducing the total consumption rate.

It is important to note that thus far, this model quantifies only the relationship between amino acid supply and consumption as a function of the ribosome copy number and states nothing about the cellular growth rate, illustrating the separation of time scales in this minimal model. With a sense of how elongation rate is tied to amino acid abundance, we now turn to how this relates to the principal cellular phenotype of this work, the cellular growth rate.

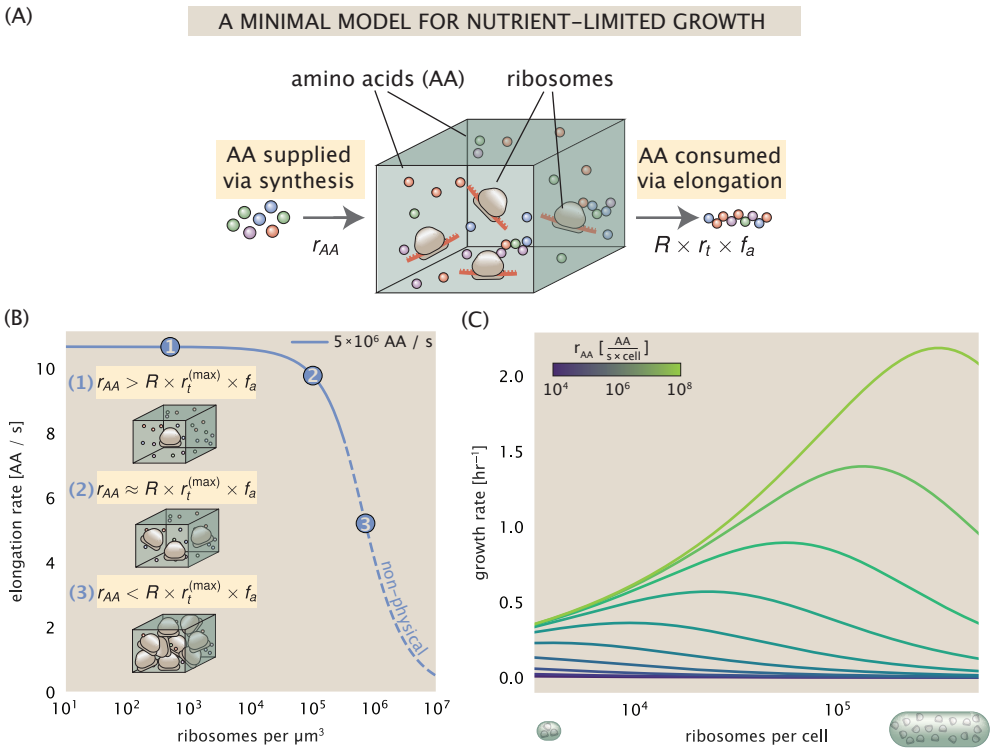

Figure 4. A minimal model for regulation of growth rate under nutrient limitation. (A) We consider a unit volume of cellular material composed of amino acids (colored spheres) provided at a supply rate r_{AA}. These amino acids are polymerized by a pool of ribosomes (brown blobs) at a rate $r_t \times R \times f_a$, where r_t is the elongation rate, R is the ribosome copy number in the unit volume, and f_a is the fraction of those ribosomes actively translating. (B) The observed elongation rate is plotted as a function of ribosomes in a unit volume μm^3. The three points correspond to three regimes of ribosome copy numbers and are shown schematically on the left-hand side. The region of the curve shown as dashed lines represents a non-physical copy number, but is shown for illustrative purposes. This curve was generated using the parameters $r_{AA} = 5 \times 10^6$ AA / s, $K_D = 5$ mM, and $r_t^{(max)} = 17.1$ AA / s. (C) The cellular growth rate is plotted as a function of total cellular ribosome copy number for different cellular amino acid supply rates, with blue and green curves corresponding to low and high supply rates, repsectively. As the ribosome copy number is increased, so too is the cell volume and total protein abundance. We direct the reader to the Suppemental Information for discussion on the inference of the realtionship between cell volume, number of peptide bonds, and ribosome copy number.

Optimal Growth Rate, Ribosomal Content, and Cell Size Depend on Nutrient Availability and Metabolic Capacity.

To relate the elongation rate to growth rate, we will constrain the set of parameters based on the growth-rate dependent proteomic changes in the available data under nutrient limitation; namely, we will restrict the values of R, N_{pep}, and V to those associated with the growth conditions observed in the amalgamated proteomic data. We will then consider how changes in the nutrient conditions, through the parameter r_{AA}, influence the maximum growth rate.

Earlier, we codified our determination of ribosome biosynthesis as the growth-rate determining cellular process in ***Equation 2*** by stating that the cellular growth rate λ was related to the ribosome abundance, elongation rate, active ribosome fraction, and the total number of peptide bonds to be formed, N_{pep}. We return to this limit in light of our expression for a condition-dependent elongation rate r_t given by ***Equation 11***. ***Figure 4***(C) shows how the observed growth rate depends on the rate of amino acid supply r_{AA} as a function of the cellular ribosome copy number. A feature immediately apparent is the presence of a maximal growth rate whose dependence on R (and consequently, the cell volume) increases with increasing r_{AA}. Importantly, however, there is an optimum set of R, N_{pep}, and V that are strictly dependent on the value of r_{AA}. Increasing the ribosomal concentration beyond the cell's metabolic capacity has the adverse consequence of depleting the supply of amino acids and a concomitant decrease in the elongation rate r_t [**??**(B)].

Of particular note is the growth rate profiles shown for low amino acid supply rates [purple and blue lines in ***Figure 4***(C)], representing growth in nutrient-poor media. In these conditions, there no longer exists a peak in growth, at least in the range of physiologically-relevant ribosome copy numbers, indicating that when conditions are particularly poor, growth can be increased by maintaining a minimal pool of active ribosomes. Depleting the ribosome pool therefore permits resources to be devoted to maintaining metabolic functions that can supply enough amino acids such that the ribosomes are elongating at a maximal rate. This observation is in agreement with the central with the central premise of the cellular resource allocation principle proposed by ***Scott et al.*** (***2010***); ***Klumpp et al.*** (***2009***); ***Klumpp and Hwa*** (***2014***); ***Hui et al.*** (***2015***).

References

Bennett, B. D., Kimball, E. H., Gao, M., Osterhout, R., Van Dien, S. J., and Rabinowitz, J. D. (2009). Absolute metabolite concentrations and implied enzyme active site occupancy in *Escherichia coli*. *Nature Chemical Biology*, 5(8):593–599.

Bremer, H. and Dennis, P. P. (2008). Modulation of Chemical Composition and Other Parameters of the Cell at Different Exponential Growth Rates. *EcoSal Plus*, 3(1).

Büke, F., Grilli, J., Lagomarsino, M. C., Bokinsky, G., and Tans, S. (2020). ppGpp is a bacterial cell size regulator. *bioRxiv*, 266:2020.06.16.154187.

Dai, X., Zhu, M., Warren, M., Balakrishnan, R., Okano, H., Williamson, J. R., Fredrick, K., and Hwa, T. (2018). Slowdown of Translational Elongation in *Escherichia coli* under Hyperosmotic Stress. - PubMed - NCBI. *mBio*, 9(1):281.

Dai, X., Zhu, M., Warren, M., Balakrishnan, R., Patsalo, V., Okano, H., Williamson, J. R., Fredrick, K., Wang, Y.-P., and Hwa, T. (2016). Reduction of translating ribosomes enables *Escherichia coli* to maintain elongation rates during slow growth. *Nature Microbiology*, 2(2):16231.

Delarue, M., Brittingham, G. P., Pfeffer, S., Surovtsev, I. V., Pinglay, S., Kennedy, K. J., Schaffer, M., Gutierrez, J. I., Sang, D., Poterewicz, G., Chung, J. K., Plitzko, J. M., Groves, J. T., Jacobs-Wagner, C., Engel, B. D., and Holt, L. J. (2018). mTORC1 Controls Phase Separation and the Biophysical Properties of the Cytoplasm by Tuning Crowding. *Cell*, 174(2):338–349.e20.

Dennis, P. P., Ehrenberg, M., and Bremer, H. (2004). Control of rRNA Synthesis in Escherichia coli: a Systems Biology Approach. *Microbiology and Molecular Biology Reviews*, 68(4):639–668.

Fernández-Coll, L., Maciag-Dorszynska, M., Tailor, K., Vadia, S., Levin, P. A., Szalewska-Palasz, A., Cashel, M., and Dunny, G. M. (2020). The Absence of (p)ppGpp Renders Initiation of *Escherichia coli* Chromosomal DNA Synthesis Independent of Growth Rates. *mBio*, 11(2):45.

Godin, M., Delgado, F. F., Son, S., Grover, W. H., Bryan, A. K., Tzur, A., Jorgensen, P., Payer, K., Grossman, A. D., Kirschner, M. W., and Manalis, S. R. (2010). Using buoyant mass to measure the growth of single cells. *Nature Methods*, 7(5):387–390.

Harris, L. K. and Theriot, J. A. (2018). Surface Area to Volume Ratio: A Natural Variable for Bacterial Morphogenesis. *Trends in microbiology*, 26(10):815–832.

Hauryliuk, V., Atkinson, G. C., Murakami, K. S., Tenson, T., and Gerdes, K. (2015). Recent functional insights into the role of (p)ppGpp in bacterial physiology. *Nature Reviews Microbiology*, 13(5):298–309.

Helmstetter, C. E. and Cooper, S. (1968). DNA synthesis during the division cycle of rapidly growing Escherichia coli Br. *Journal of Molecular Biology*, 31(3):507–518.

Hui, S., Silverman, J. M., Chen, S. S., Erickson, D. W., Basan, M., Wang, J., Hwa, T., and Williamson, J. R. (2015). Quantitative proteomic analysis reveals a simple strategy of global resource allocation in bacteria. *Molecular Systems Biology*, 11(2):e784–e784.

Klumpp, S. and Hwa, T. (2014). Bacterial growth: Global effects on gene expression, growth feedback and proteome partition. *Current Opinion in Biotechnology*, 28:96–102.

Klumpp, S., Zhang, Z., and Hwa, T. (2009). Growth Rate-Dependent Global Effects on Gene Expression in Bacteria. *Cell*, 139(7):1366–1375.

Kraemer, J. A., Sanderlin, A. G., and Laub, M. T. (2019). The Stringent Response Inhibits DNA Replication Initiation in E. coliby Modulating Supercoiling of oriC. *mBio*, 10(4):822.

Maaløe, O. (1979). *Regulation of the Protein-Synthesizing Machinery—Ribosomes, tRNA, Factors, and So On*. Gene Expression. Springer.

Milo, R., Jorgensen, P., Moran, U., Weber, G., and Springer, M. (2010). BioNumbers—the database of key numbers in molecular and cell biology. *Nucleic Acids Research*, 38(suppl_1):D750–D753.

Roller, B. R. K., Stoddard, S. F., and Schmidt, T. M. (2016). Exploiting rRNA operon copy number to investigate bacterial reproductive strategies. *Nature microbiology*, 1(11):1–7.

Schaechter, M., MaalØe, O., and Kjeldgaard, N. O. (1958). Dependency on Medium and Temperature of Cell Size and Chemical Composition during Balanced Growth of *Salmonella typhimurium*. *Microbiology*, 19(3):592–606.

Schmidt, A., Kochanowski, K., Vedelaar, S., Ahrné, E., Volkmer, B., Callipo, L., Knoops, K., Bauer, M., Aebersold, R., and Heinemann, M. (2016). The quantitative and condition-dependent *Escherichia coli* proteome. *Nature Biotechnology*, 34(1):104–110.

Scott, M., Gunderson, C. W., Mateescu, E. M., Zhang, Z., and Hwa, T. (2010). Interdependence of cell growth and gene expression: origins and consequences. *Science*, 330(6007):1099–1102.

Si, F., Li, D., Cox, S. E., Sauls, J. T., Azizi, O., Sou, C., Schwartz, A. B., Erickstad, M. J., Jun, Y., Li, X., and Jun, S. (2017). Invariance of Initiation Mass and Predictability of Cell Size in *Escherichia coli*. *Current Biology*, 27(9):1278–1287.

Soler-Bistué, A., Aguilar-Pierlé, S., Garcia-Garcerá, M., Val, M.-E., Sismeiro, O., Varet, H., Sieira, R., Krin, E., Skovgaard, O., Comerci, D. J., Eduardo P. C. Rocha, and Mazel, D. (2020). Macromolecular crowding links ribosomal protein gene dosage to growth rate in Vibrio cholerae. *BMC Biology*, 18(1):1–18.

Taheri-Araghi, S., Bradde, S., Sauls, J. T., Hill, N. S., Levin, P. A., Paulsson, J., Vergassola, M., and Jun, S. (2015). Cell-size control and homeostasis in bacteria. - PubMed - NCBI. *Current Biology*, 25(3):385–391.

Zhu, M. and Dai, X. (2019). Growth suppression by altered (p)ppGpp levels results from non-optimal resource allocation in *Escherichia coli*. *Nucleic Acids Research*, 47(9):4684–4693.